Applied Mathematics and Computation 221 (2013) 424–432

Contents lists available at SciVerse ScienceDirect

Applied Mathematics and Computation

journal homepage: www.elsevier.com/locate/amc

Proving the non-degeneracy of the longest-edge trisection by a space of triangular shapes with hyperbolic metric

Francisco Perdomo, Ángel Plaza *

Department of Mathematics, University of Las Palmas de Gran Canaria, 35017 Las Palmas de Gran Canaria, Spain

ARTICLE INFO

Keywords:
Triangle subdivision
Trisection
Finite element method
Mesh quality

ABSTRACT

From an initial triangle, three triangles are obtained joining the two equally spaced points of the longest-edge with the opposite vertex. This construction is the base of the longest-edge trisection method. Let Δ be an arbitrary triangle with minimum angle α. Let Δ' be any triangle generated in the iterated application of the longest-edge trisection. Let α' be the minimum angle of Δ'. Thus $\alpha' \geqslant \alpha/c$ with $c = \frac{\pi/3}{\arctan\left(\sqrt{3}/11\right)}$ is proved in this paper. A region of the complex half-plane, endowed with the Poincare hyperbolic metric, is used as the space of triangular shapes. The metric properties of the piecewise-smooth complex dynamic defined by the longest-edge trisection are studied. This allows us to obtain the value c.

1. Introduction

Partition methods are employed frequently to obtain mesh refinements [4,9,10,12,13]. Partitions and local refinement algorithms are related [9]. For example, a local refinement has recently been proposed, based on LE trisection [6]. Also the seven-triangle longest edge partition is related to the LE trisection [3,7]. This work refers to the longest-edge (LE) trisection method for triangles [5,6]. In any triangle there is obviously a longest edge and, on this edge there are two points which divide it into three equal parts. The LE-trisection of the triangle is obtained by joining these two points with the opposite vertex to the longest edge. Three new smaller triangles are obtained. The LE-trisection can be applied iteratively (see Fig. 1). In this way, refinements of any partition can be obtained at very low cost. That is interesting for example in finite element methods, but some conditions should be satisfied. One of these conditions is that the triangles generated in the procedure should not degenerate. This means that the smallest angles have a lower bound which only depends on the initial triangles [11].

In this paper, it is proved that the smallest angles do not drop from the initial minimum angle divided by a constant approximately equal to 6.7052. The main result is the following

Theorem 1. *Let α be the smallest angle of a triangle. If the longest-edge trisection is iteratively applied to this initial triangle, then the smallest angle α' of any triangle generated satisfies $\alpha' \geqslant \alpha/c$, where $c = \frac{\pi/3}{\arctan\left(\sqrt{3}/11\right)}$.* □

There is solid empirical evidence for Theorem 1 in the paper by Plaza et al. [5]. In the present work, a proof of this theorem is given by studying the discrete dynamical system defined by the longest-edge trisection in a space of triangular shapes with hyperbolic metric.

* Corresponding author.
E-mail address: aplaza@dmat.ulpgc.es (Á. Plaza).

0096-3003/$ - see front matter © 2013 Elsevier Inc. All rights reserved.
http://dx.doi.org/10.1016/j.amc.2013.06.075

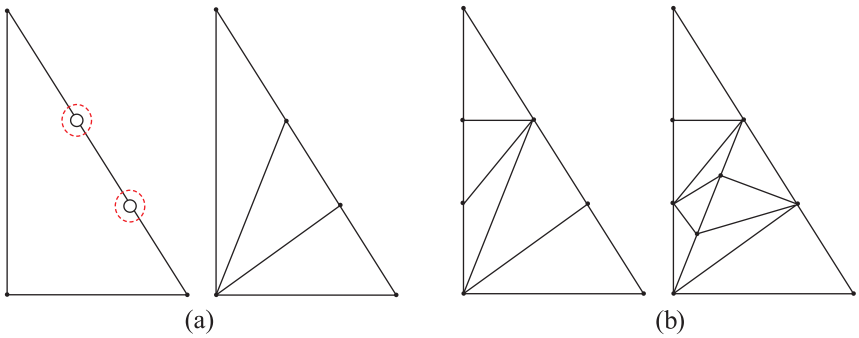

Fig. 1. (a) Longest-edge trisection of a triangle. (b) 2nd and 3rd iteration.

2. Space of triangles and LE-trisection dynamic

By scaling, symmetries, translations and rotations, a normalized triangle can be associated to any triangle. A normalized triangle has the two vertices of the longest edge attached to 0 and 1, the opposite vertex to the longest edge on the upper half plane $\mathrm{Im}\, z > 0$ and the shortest edge on the left of $\mathrm{Re}\, z = \frac{1}{2}$. Then there is a bijection between the points in the region $\Sigma = \{z/\mathrm{Im}\, z > 0,\ \mathrm{Re}\, z \leqslant \frac{1}{2},\ |z-1| \leqslant 1\}$ and similar triangles (see Fig. 2(a)). The region Σ is called the space of triangular shapes [2,8].

For a normalized triangle, three triangles are obtained by the longest-edge (LE) trisection: they are called the left, middle and right triangles. The left triangle Δ_L is the triangle with vertices 0, $\frac{1}{3}$ and z. The middle triangle Δ_M is the triangle with vertices $\frac{1}{3}$, $\frac{2}{3}$ and z. Finally the right (on account of its position) triangle Δ_R is the triangle with vertices $\frac{2}{3}$, 1 and z (see Fig. 2(b)). The normalization of the left triangle Δ_L gives a complex number $W_L(z)$ (see Fig. 3). A complex function can be defined if this complex number is associated to z. Then the left function W_L is defined as the function of the region Σ into itself with $z \mapsto W_L(z)$, where z is the complex number associated to the initial triangle Δ in the normalized position, and $W_L(z)$ is the complex number associated to the left triangle Δ_L by the normalization procedure. In the same way, the middle function W_M and the right function W_R are defined. Therefore the normalization reduces the LE-trisection method to the discrete dynamic in the space of triangles Σ associated to the three complex functions W_L, W_M and W_R.

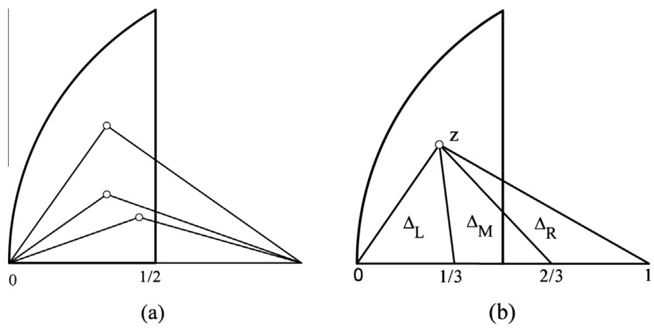

Fig. 2. (a) Three triangles in normalized position. (b) Left, middle and right triangles obtained by longest-edge trisection.

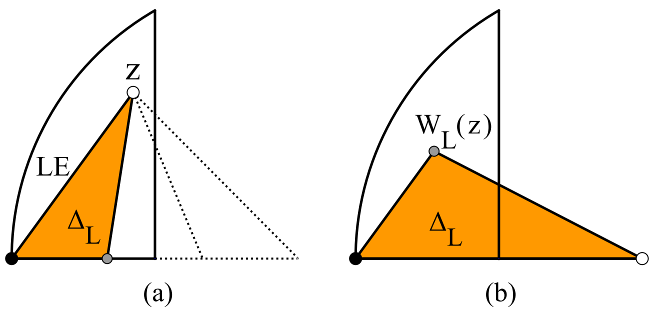

Fig. 3. (a) The left triangle Δ_L before the normalization procedure. (b) The left triangle Δ_L in the normalized position associated to $W_L(z)$.

The normalization procedure of Δ_L, Δ_M and Δ_R depends on the relative position of the longest, middle and shortest edges. Therefore the functions W_L, W_M and W_R are piecewise functions.

An example of how the definitions of these piecewise functions can be obtained follows. Let z in Σ be such that $\mathrm{Re}\, z \geqslant \frac{1}{6}$ and $|z-\frac{1}{3}| \geqslant \frac{1}{3}$ (in color in Fig. 4(a)). The normalization of the triangle 0, $\frac{1}{3}$ and z defines the point $W_L(z)$. A rotation is used, together with scaling and the complex conjugation as shown in Fig. 4(b)–(d). In this case $W_L(z) = \frac{1}{3\bar{z}}$ is obtained.

For a fixed metric relation of the initial edges, the normalization procedure is composed of scaling and movements of planes, together possibly with symmetry. Then the definitions of the piecewise functions W_L, W_M and W_R are Möbius functions, possibly combined with conjugate complex function. The complete definitions of W_L, W_M and W_R are given in Fig. 5.

3. Hyperbolic metric in the space of triangles

Some facts about hyperbolic geometry, and specifically about the Poincare half-plane model, are naturally related to the LE-trisection dynamic in the space of triangular shapes. In the Poincare half-plane, the points are complex numbers with $\mathrm{Im}\, z > 0$, and the geodesics are semi-circumferences and the straight lines which are orthogonal to $\mathrm{Im}\, z = 0$ (see [1] for a survey). The isometries in the half-plane have expressions such as $\frac{az+b}{cz+d}$ or $\frac{a(-\bar{z})+b}{c(-\bar{z})+d}$ with real coefficients verifying $a \cdot d - b \cdot c > 0$. Note that the expressions of W_L, W_M and W_R are isometries (see Fig. 5). Moreover the lines delimiting the regions on the definition of W_L, W_M and W_R are geodesics (see Fig. 6).

Lemma 2. *Let W be any of the functions W_L, W_M and W_R. Then W is invariant under inversion with respect to the circumferences (or under symmetry with respect to the straight line) which appear in its definition.*

Proof. For example, let $W = W_D$. The inversion with respect to $\left|z-\frac{2}{3}\right| = \frac{1}{3}$ is $\frac{2\bar{z}-1}{3\bar{z}-2}$. Its composition with $\frac{-1}{3z-3}$ is $\frac{3\bar{z}-2}{3\bar{z}-3}$. Or another example, let $W = W_L$. The symmetry with respect to $\mathrm{Re}\, z = 1/6$ is given by $z \mapsto \frac{1}{3} - \bar{z}$. The composition of this symmetry with the expression $\frac{-1}{3z-1}$ (resp. $\frac{3\bar{z}}{3\bar{z}-1}$, $3z$) results $\frac{1}{3\bar{z}}$ (resp. $\frac{3z-1}{3z}$, $1-3\bar{z}$). □

In the Poincare half-plane the hyperbolic distance d between z_1 and z_2 is defined by the formula

$$\cosh d = 1 + \frac{|z_1 - z_2|^2}{2 \cdot \mathrm{Im}\, z_1 \cdot \mathrm{Im}\, z_2}. \tag{1}$$

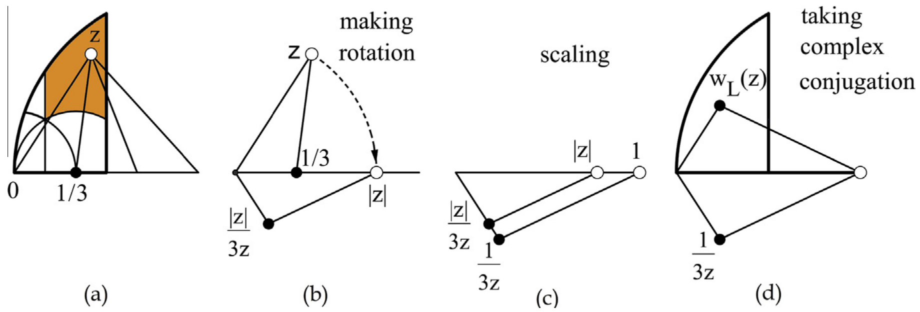

Fig. 4. The procedure to obtain the expression of W_R for z in the coloured region. (For interpretation of the references to colour in this figure legend, the reader is referred to the web version of this article.)

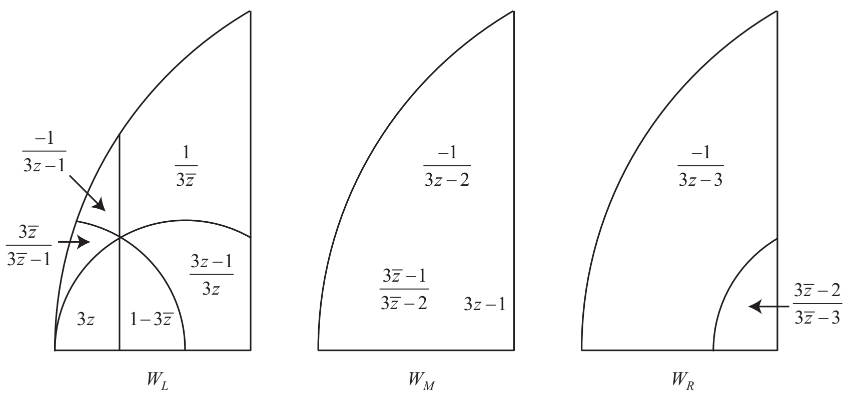

Fig. 5. Piecewise expressions of the functions W_L, W_M and W_R.

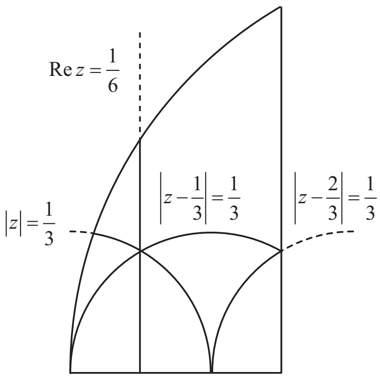

Fig. 6. Lines delimiting the regions on the definitions of W_L, W_M and W_R.

The following property asserts that the three functions W_L, W_M and W_R do not increase the distance between points in the space of triangles.

Lemma 3 (*non-increasing property*). *Let W be any of the functions W_L, W_M and W_R. For every z_1 and z_2 in the space of triangles*

$$d(W(z_1), W(z_2)) \leqslant d(z_1, z_2),$$

where $d(\cdot,\cdot)$ denotes the hyperbolic distance in the Poincare half-plane.

Proof. If z_1 and z_2 are in a region with the same definition of W, then $d(z_1, z_2) = d(W(z_1), W(z_2))$, because W is an isometry in the half-plane hyperbolic model. In another case, due to the symmetries of W, z_1' and z_2' exist in the normalized region with $W(z_1) = W(z_1')$ and $W(z_2) = W(z_2')$, z_1' and z_2' in a zone with same expression of W and, finally, with $d(z_1', z_2') < d(z_1, z_2)$. Thus

$$d(W(z_1), W(z_2)) = d(W(z_1'), W(z_2')) = d(z_1', z_2') < d(z_1, z_2)$$

and the lemma follows. □

Remark. It follows from the proof that strict inequality occurs if, and only if, z_1 and z_2 are not in the same region of definition of W.

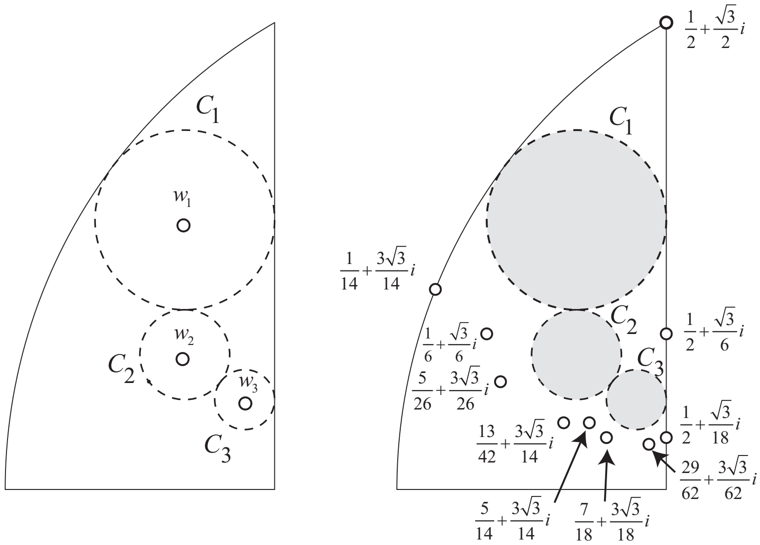

Fig. 7. (a) Circles C_1, C_2 and C_3 with hyperbolic centres ω_1, ω_2 and ω_3 (points in white) and with radius $\ln\sqrt{2}$. (b) Points in the orbit of $z_{eq} = \frac{1}{2} + \frac{\sqrt{3}}{2}i$ outside the circles C_1, C_2 and C_3.

4. Orbits and closed sets for longest-edge trisection

From an initial complex number z in the space of triangles Σ, images with left, middle and right functions can be obtained. Functions $W_L,\ W_M$ and W_R can be applied iteratively. If z is in Σ, let the orbit of z be set Γ_z consisting of z and its successive images through $W_L,\ W_M$ and W_R. For example if $\omega_1 = \frac{1}{3} + \frac{\sqrt{2}}{3} i$, then its orbit is $\Gamma_{\omega_1} = \{\omega_1, \omega_2, \omega_3\}$, where $\omega_2 = \frac{1}{3} + \frac{\sqrt{2}}{6} i$ and $\omega_3 = \frac{4}{9} + \frac{\sqrt{2}}{9} i$ (see Fig. 7(a)).

A subset Ω of the space of triangles Σ is a closed set for LE-trisection, or simply a closed set, if for z in Ω, then $W_L(z),\ W_M(z)$ and $W_R(z)$ are in Ω. If z is in a closed region, then its orbit Γ_z is included within the closed region.

Outside the orbits there are other closed sets. The following corollary of the non-increasing property gives some examples that will be used later on.

Corollary 4. *Let z be a complex number in the space of triangles Σ. Let Ω be the intersection with Σ of the union of the hyperbolic circles with centres in Γ_z and with the same radius r. Then Ω is a closed set for the LE-trisection.*

Proof. Let w be in Ω. By definition there exists a z' in Γ_z with $d(w, z') \leqslant r$. If W is any of the functions $W_L,\ W_M$ and W_R, by the non-increasing property, then $d(W(w), W(z')) \leqslant r$. So $W(w)$ is within Ω because $W(z')$ is within Γ_z. □

For example, the union of the three circles $C_1,\ C_2$ and C_3 with hyperbolic centres $\omega_1,\ \omega_2$ and ω_3, respectively, and with radius $\ln\sqrt{2}$ is a closed set (see Fig. 7(a)).

The complex number associated with the equilateral triangle is $z_{eq} = \frac{1}{2} + \frac{\sqrt{3}}{2} i$. Its orbit $\Gamma_{z_{eq}}$ has a finite number of points outside the circles $C_1,\ C_2$ and C_3 which are represented in Fig. 7(b). They can be obtained using the definition of $W_L(z),\ W_M(z)$ and $W_R(z)$ given in Fig. 4. If any point is inside the circles $C_1,\ C_2$ and C_3, also its images are inside the circles $C_1,\ C_2$ and C_3, and it is not necessary to evaluate it.

5. Proof of the Theorem 1

In the LE-trisection dynamic, the non-degeneracy property has the following setting. Let z be within the space of triangular shapes Σ. Let z' be in the orbit of z. Let α and α' be the arguments of $1-\bar{z}$ and $1-\bar{z}'$, respectively. If the maximum c of the quotient α/α' is evaluated in Σ, then $\alpha' \geqslant \alpha/c$ for every z in the space of triangular shapes Σ.

To evaluate the maximum of α/α', the space of triangles Σ is covered with two overlapping regions Ω_1 and Ω_2. To define Ω_1, tangent geodesics are traced to the circles $C_1,\ C_2$ and C_3 from the points in $\Gamma_{z_{eq}}$ which are outside the circles. Ω_1 is composed of the circles $C_1,\ C_2$ and C_3 and the regions which are tangent cones between the geodesics (see Fig. 8(a)). Let Ω_2 be the region in Σ under the circles $C_1,\ C_2$ and C_3 (see Fig. 8(b)).

Lemma 5. *Ω_1 is a closed region.*

Proof. The union of $C_1,\ C_2$ and C_3 is a closed region. It is sufficient to see that the image of every tangent cone for $W_L,\ W_M$ or W_R is included within Ω_1. If the restriction to a tangent cone of $W_L,\ W_M$ or W_R is a Möbius function and the image of base point of the tangent cone is within $\Gamma_{z_{eq}}$, the image of the tangent cone is also a tangent cone. This is because Möbius maps transform circumferences into circumferences, and preserve angles, incidences and tangents.

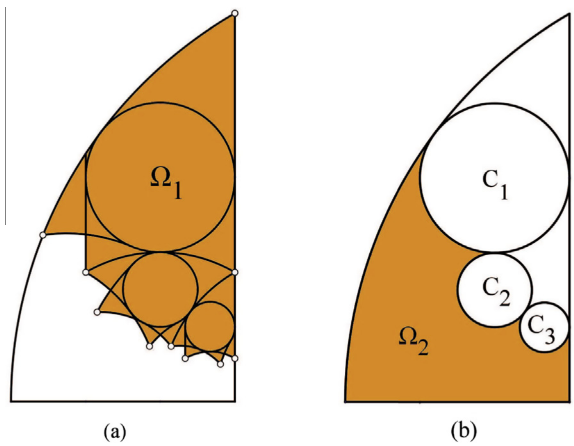

Fig. 8. The space of triangles Σ splits into two overlapping regions Ω_1 and Ω_2.

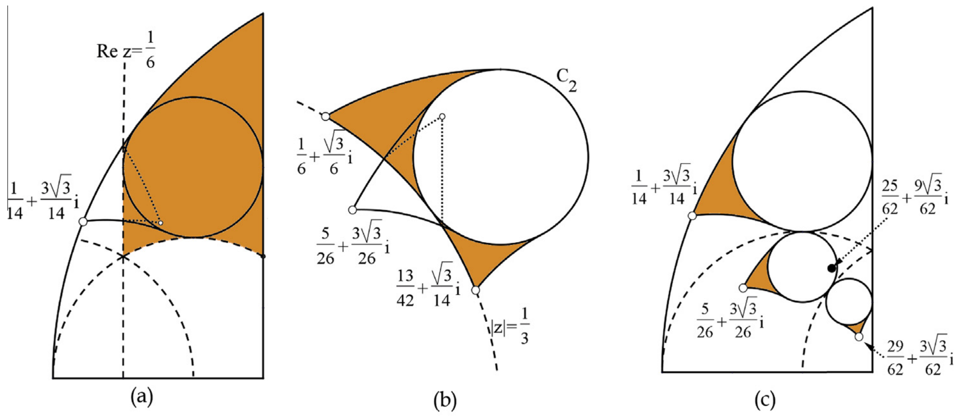

Fig. 9. (a) and (b) Tangent cones with two definitions of W_L. (c) Tangent cones with base point mapped into C_2 by W_M.

The only function for which the restriction to a tangent cone has two different expressions is W_L. This only happens for the two tangent cones with base points $\frac{1}{14}+\frac{3\sqrt{3}}{14}i$ and $\frac{5}{26}+\frac{3\sqrt{3}}{26}i$ (see Fig. 9(a) and (b)).

We consider first the cone with base point $\frac{1}{14}+\frac{3\sqrt{3}}{14}i$. See Fig. 9(a). Due to the symmetry of W_L with respect to the boundary line $x=\frac{1}{6}$, the image of this tangent cone is included within the image of a region where $W_L(z)=\frac{1}{3\bar{z}}$, which is an involution.

For the second point $\frac{5}{26}+\frac{3\sqrt{3}}{26}i$, due to the symmetry of W_L with respect to the boundary circumference $|z|=\frac{1}{3}$, the image of this tangent cone is included within the images of two other tangent cones and the circle C_2, which are in Ω_1. See Fig. 9(b).

It may also happen that the image of the base point is in $C_1,\ C_2$ or C_3. This happens for function W_M and the tangent cones with base points $\frac{1}{14}+\frac{3\sqrt{3}}{14}i,\ \frac{5}{26}+\frac{3\sqrt{3}}{26}i$ or $\frac{29}{62}+\frac{3\sqrt{3}}{62}i$. The image of these three points is $\frac{25}{62}+\frac{9\sqrt{3}}{62}i$ which is inside C_2. See Fig. 9(c). Since the restriction of W_M to tangent cones is a möbius map, then the images of tangent cones are tangent cones to C_1 with base point $\frac{25}{62}+\frac{9\sqrt{3}}{62}i$. In any case the images are in Ω_1. □

Since Ω_1 is a closed region, then $\alpha/\alpha' \leqslant c$ with $c=\frac{\pi/3}{\arctan(\sqrt{3}/11)}\approx 6.7052$, because for z in Ω_1, the maximum and the minimum arguments of $1-\bar{z}$ are $\frac{\pi}{3}$ and $\arctan\left(\frac{\sqrt{3}}{11}\right)$, respectively. The bound is accurate because $\frac{29}{62}+\frac{3\sqrt{3}}{62}i$ and $\frac{7}{18}+\frac{\sqrt{3}}{18}i$ are in $\Gamma_{z_{eq}}$ (See Fig. 10).

However Ω_2 is not a closed region. Nevertheless an upper bound c' of α/α' in Ω_2 will be obtained as follows. Let $r>\ln\sqrt{2}$ and let γ_r be the line composed by the arcs of circumferences in Ω_2 with centers in the points of Γ_{ω_1} and radius r (see Fig. 11).

Lemma 6. *For the points in γ_r the maximum argument of $1-\bar{z}$ is obtained for z_1 at the top of γ_r. The minimum is obtained for z_2 in the arc of γ_r with the centre in ω_3 whose tangent goes through $1=1+0i$ (see Fig. 11(a)).*

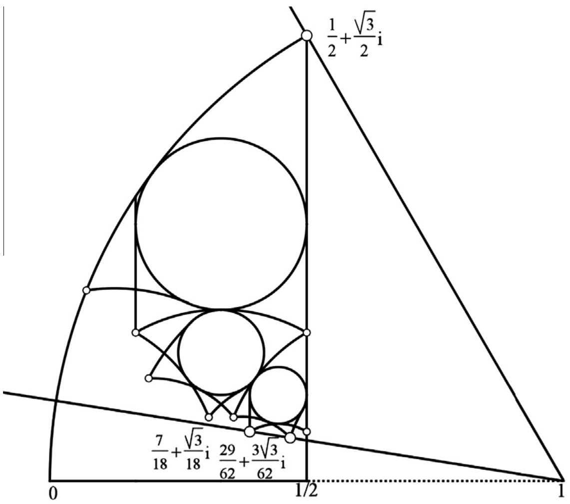

Fig. 10. Closed region Ω_1 and the top and bottom tangents from the point $1=1+0i$.

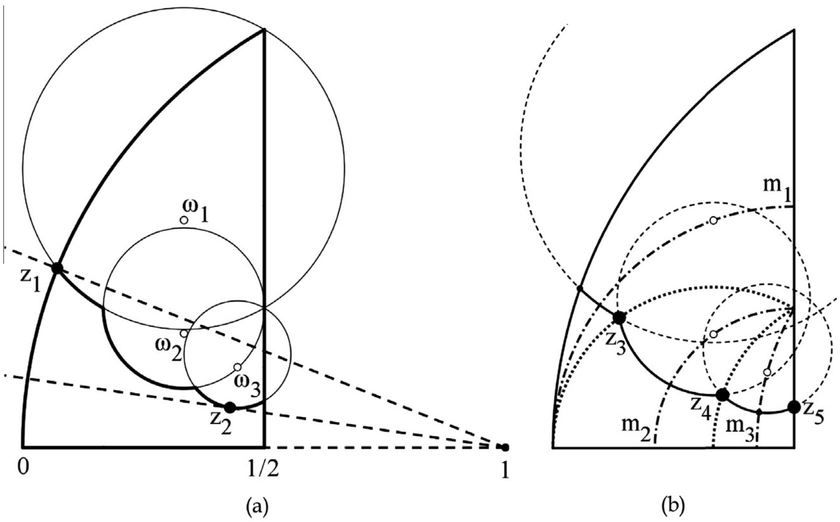

Fig. 11. γ_r is composed by arcs with hyperbolic centers in $\omega_1,\ \omega_2$ and ω_3 and the same radius r.

Proof. Let z_3 be the intersection of the arcs of γ_r with centres in ω_1 and ω_2. Point z_3 is on the circumference $|z-\frac{1}{3}|=\frac{1}{3}$ which is the hyperbolic perpendicular bisector of the segment from ω_1 to ω_2 (see Fig. 11(b)). Let m_1 be the geodesic which equation $|z-\frac{1}{2}|=\frac{1}{2}$. Inversion with respect to m_1 preserves the distance to ω_1 which is in m_1. Furthermore, inversion with respect to m_1 applies the circumference $|z-\frac{1}{3}|=\frac{1}{3}$ to $|z-1|=1$. So z_1 is the inversion of z_3 with respect to m_1, and $z_1,\ z_3$ and $\frac{1}{2}$ are aligned.

With similar arguments it is proved that z_3 is the inversion of z_4 with respect to m_2, and z_4 is the inversion of z_5 with respect to m_3, where m_2 and m_3 are the geodesics $|z-\frac{1}{2}|=\frac{\sqrt{3}}{6}$ and $|z-1|=\frac{1}{\sqrt{3}}$, respectively, which are shown in Fig. 11. Then $z_3,\ z_4$ and $\frac{1}{2}$ are aligned, and $z_4,\ z_5$ and 1 are aligned. Hence $z_3,\ z_4$ and z_5 are under the segment from z_1 to $1=1+0i$.

In addition, z_2 gives the minimal argument for $1-\bar{z}$ in γ_r, because the circumference with center ω_3 is the lowest of the three circumferences. □

The following proposition gives a result which will be used later on.

Lemma 7. *If z_1 is the top point directly over the centre of the geodesic, the hyperbolic length of the segment from z_0 in the geodesic to z_1, say l, verifies*

$$\frac{\theta}{2}=\arctan\left(e^{-l}\right) \tag{2}$$

where θ is the difference between $\pi/2$ and the central angle determined by the segment from z_0 to z_1 over the geodesic.

Proof. Locally the hyperbolic metric is defined by $ds^2=\frac{dx^2+dy^2}{y^2}$. Then $l=\int_{[z_0,z_1]}ds=\int_\theta^{\pi/2}\frac{r\cdot d\beta}{r\sin(\beta)}=-\ln\left(\tan\left(\frac{\theta}{2}\right)\right)$ (see Fig. 12). □

Lemma 8. *Let z be in Ω_2 and z' in the orbit of z. Let α and α' be the arguments of $1-\bar{z}$ and $1-\bar{z}'$, respectively. There is a constant $c'<c$ with $\alpha'\geqslant\alpha/c'$.*

Proof. For every z in Ω_2, there is a radius $r>\ln\sqrt{2}$ with z in γ_r. By the non-decreasing property, if z' is in the orbit Γ_z, the distance of z' to one of the points in Γ_{ω_1} is less or equal than r. Obviously, the worst case for degeneracy occurs when z' is over the curve γ_r. It can be supposed that α and α' are the arguments of $1-\bar{z_1}$ and $1-\bar{z_2}$ respectively, where z_1 and z_2 are as in the previous lemma.

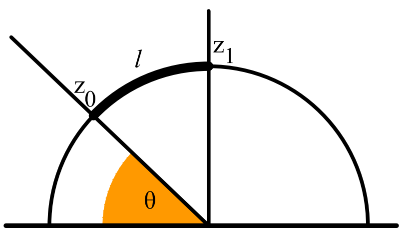

Fig. 12. Illustrative figure for Lemma 7

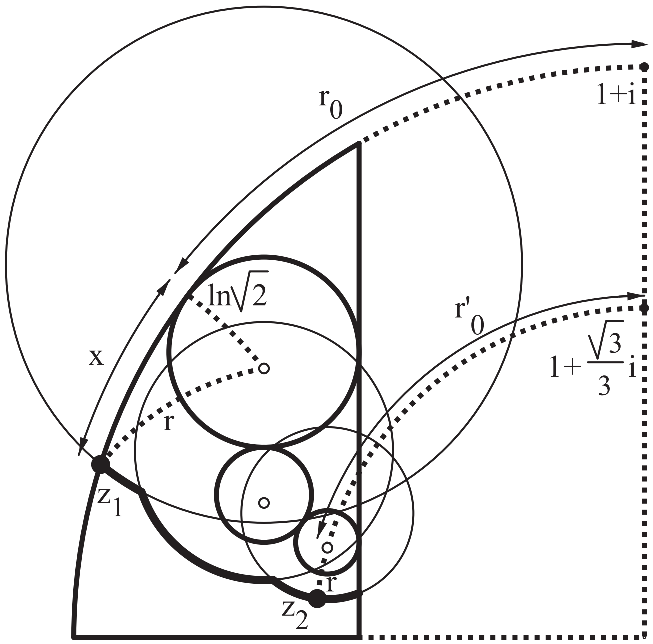

Fig. 13. Set γ_r for $r > \ln\sqrt{2}$ and critical point z_1 and z_2.

The tangency point between the arc in $|z-1|=1$ of the region Σ and circumference C_1 is $\frac{1}{5}+\frac{3}{5}i$. Let x be the distance from z_1 to the tangency point $\frac{1}{5}+\frac{3}{5}i$ (see Fig. 13). Let r_0 be the distance from the tangency point to the point $1+i$. By Eq. (2) then $\frac{\alpha}{2}=\arctan\left(e^{-x-r_0}\right)$.

Let r_0' be the distance from the point ω_3 to the point $1+\frac{\sqrt{3}}{3}i$, the top point in the geodesic through ω_3 with center $1=1+0i$. The point z_2 lies over this geodesic $|z-1|=\frac{1}{\sqrt{3}}$, and its distance r to ω_3 can be added to r_0'. $\frac{\alpha'}{2}=\arctan\left(e^{-r-r_0'}\right)$ is also obtained by Eq. (2).

Therefore

$$\frac{\alpha}{\alpha'}=\frac{\arctan\left(e^{-x-r_0}\right)}{\arctan\left(e^{-r-r_0'}\right)}<\frac{e^{-x-r_0}}{\frac{\pi}{4}e^{-r-r_0'}}$$

because function $\arctan x$ verifies the inequalities $\frac{\pi}{4}x<\arctan x<x$ if $0<x<1$. Then the expression $e^{(r-x)+(r_0'-r_0)}$ must be bounded. Using Formula (1) it follows that $\cosh r_0=\frac{5}{3}$ and $\cosh r_0'=\frac{3\sqrt{6}}{2}$. Consequently, $e^{r_0}=3$, $e^{r_0'}=\frac{5\sqrt{2}+3\sqrt{6}}{2}$, and thus $e^{r_0'-r_0}=\frac{5\sqrt{2}+3\sqrt{6}}{6}$.

Otherwise $\cosh x\cdot\cosh(\ln\sqrt{2})=\cosh r$ by the hyperbolic version of the Pythagoras theorem. Then $\cosh x=\frac{2\sqrt{2}}{3}\cosh r$ and

$$e^{r-x}=\frac{e^r}{\frac{2\sqrt{2}}{3}\cosh r+\sqrt{\frac{8}{9}\cosh^2 r-1}}\leqslant\frac{e^r}{\frac{2\sqrt{2}}{3}\cosh r+\frac{2\sqrt{2}}{3}\cosh r-1}=\frac{3e^r}{4\sqrt{2}\cosh r-3}.$$

But the maximum value of function $\frac{3e^r}{4\sqrt{2}\cosh r-3}$ $\frac{24\sqrt{2}}{23}$.

Finally

$$\frac{\alpha}{\alpha'}<\frac{4}{\pi}\cdot 24\sqrt{2}/23\cdot\frac{5\sqrt{2}+3\sqrt{6}}{6}\approx 4.5155.\qquad\Box$$

6. Conclusion

In this paper a region of the upper half complex plane has been used as the space of triangular shapes. In a natural way this space has been endowed with hyperbolic metric. The properties of the piecewise-smooth discrete dynamic induced by LE-trisection in this space of triangular shapes has been studied. It has allowed us to obtain the lower bound for the smallest angle obtained by the iterative application of the LE-trisection.

Acknowledgment

This work has been supported in part by Project number MTM2008-05866-C03-02/MTM from the Spanish Ministerio de Educación y Ciencia.

References

[1] J. Anderson, Hyperbolic Geometry, Springer, 2005.
[2] C. Gutiérrez, F. Gutiérrez, M.-C. Rivara, Complexity of bisection method, Theor. Comput. Sci. 382 (2) (2007) 131–138.
[3] A. Márquez, A. Moreno-González, A. Plaza, J.P. Suárez, The seven-triangle longest-side partition of triangles and mesh quality improvement, Finte Elem. Anal. Des. 44 (12–13) (2008) 748–758.
[4] A. Plaza, G.F. Carey, Local refinement of simplicial grids based on the skeleton, Appl. Numer. Math. 32 (2) (2000) 195–218.
[5] A. Plaza, S. Falcón, J.P. Suárez, On the non-degeneracy property of the longest-edge trisection of triangles, Appl. Math. Comput. 216 (3) (2010) 862–869.
[6] A. Plaza, S. Falcón, J.P. Suárez, P. Abad, A local refinement algorithm for the longest-edge trisection of triangle meshes, Math. Comput. Simul. 82 (12) (2012) 2971–2981.
[7] A. Plaza, A. Márquez, A. Moreno-González, J.P. Suárez, Local refinement based on the 7-triangle longest-edge partition, Math. Comput. Simul. 79 (8) (2009) 2444–2457.
[8] A. Plaza, J.P. Suárez, G.F. Carey, A geometric diagram and hybrid scheme for triangle subdivision, Comput. Aided Geom. Des. 24 (1) (2007) 19–27.
[9] M.-C. Rivara, Mesh refinement processes based on the generalized bisection of simplices, SIAM J. Numer. Anal. 21 (3) (1984) 604–613.
[10] M.-C. Rivara, Local modification of meshes for adaptive and/or multigrid finite-element methods, J. Comput. Appl. Math. 36 (1) (1991) 79–89.
[11] I.G. Rosenberg, F. Stenger, A lower bound on the angles of triangles constructed by bisecting the longest side, Math. Comput. 29 (130) (1975) 390–395.
[12] J.P. Suárez, A. Plaza, Four-triangles adaptive algorithms for RTIN terrain meshes, Math. Comput. Model. 49 (5) (2009) 1012–1029.
[13] O. Zienkiewicz, J. Zhu, Adaptivity and mesh generation, Int. J. Numer. Methods Eng. 32 (4) (1991) 783–810.